Indonesian Journal of Electrical Engineering and Computer Science
Vol. 11, No. 1, July 2018, pp. 60~73
ISSN: 2502-4752, DOI: 10.11591/ijeecs.v11.i1.pp60-73

Advanced Active Power Filter Performance for Grid Integrated Hybrid Renewable Power Generation Systems

S. Guru Prasad[1], K S Srikanth[2], B V Rajanna[3]
[1] Department of Electrical and Electronics Engineering, Research Scholar, K L E F, Vaddeswaram, Guntur, A.P., India
[2,3] Department of Electrical and Electronics Engineering, K L E F, Vaddeswaram, Guntur, A.P., India

Article Info

Article history:

Received Jan 12, 2018
Revised Mar 30, 2018
Accepted Apr 19, 2018

Keywords:

Active power filter
Current control
Four-leg converters
Predictive control
Matlab/simulink

ABSTRACT

An active power filter implemented with a four leg voltage-source inverter using a predictive control scheme is presented. The use of a four leg voltage-source inverter allows the compensation of current harmonic components, as well as unbalanced current generated by single-phase nonlinear loads. A detailed yet simple mathematical model of the active power filter, including the effect of the equivalent power system impedance, is derived and used to design the predictive control algorithm. The compensation performance of the proposed active power filter and the associated control scheme under steady state and transient operating conditions is demonstrated through simulations and experimental results.

Corresponding Author:

K S Srikanth,
Department of Electrical and Electronics Engineering,
Koneru Lakshmaiah Education Foundation, Green Fields,Vaddeswaram,
Guntur District, A.P., India, Pincode: 522502.
Email: srikanth.dsd@gmail.com

1. INTRODUCTION

Renewable generation affects power quality due to its nonlinearity, since solar generation plants and wind power generators must be connected to the grid through high-power static PWM converters [1]. The non uniform nature of power generation directly affects voltage regulation and creates voltage distortion in power systems. This new scenario in power distribution systems will require more sophisticated compensation techniques. Although active power filters implemented with three-phase four-leg voltage-source inverters (4L-VSI) have already been presented in the technical literature [2]-[6], the primary contribution of this paper is a predictive control algorithm designed and implemented specifically for this application. Traditionally, active power filters have been controlled using pre-tuned controllers, such as PI-type or adaptive, for the current as well as for the dc-voltage loops [7],[8]. PI controllers must be designed based on the equivalent linear model, while predictive controllers use the nonlinear model, which is closer to real operating conditions. An accurate model obtained using predictive controllers improves the performance of the active power filter, especially during transient operating conditions, because it can quickly follow the current-reference signal while maintaining a constant dc-voltage.

So far, implementations of predictive control in power converters have been used mainly in induction motor drives [9]-[16]. In the case of motor drive applications, predictive control represents a very intuitive control scheme that handles multivariable characteristics, simplifies the treatment of dead-time compensations, and permits pulse-width modulator replacement. However, these kinds of applications present disadvantages related to oscillations and instability created from unknown load parameters [17]-[26]. One advantage of the proposed algorithm is that it fits well in active power filter applications, since the power converter output parameters are well known [26]-[30]. These output parameters are obtained from the

converter output ripple filter and the power system equivalent impedance. The converter output ripple filter is part of the active power filter design and the power system impedance is obtained from well-known standard procedures [18]-[35]. In the case of unknown system impedance parameters, an estimation method can be used to derive accurate *R–L* equivalent impedance model of the system [31]-[40]. This paper presents the mathematical model of the 4L-VSI and the principles of operation of the proposed predictive control scheme, including the design procedure [40]-[58]. The complete description of the selected current reference generator implemented in the active power filter is also presented. Finally, the proposed active power filter and the effectiveness of the associated control scheme compensation are demonstrated through simulation and validated with experimental results obtained in a 2 kVA laboratory prototype.

2. FOUR-LEG CONVERTER MODEL

Figure 1 shows the configuration of a typical power distribution system with renewable power generation. It consists of various types of power generation units and different types of loads. Renewable sources, such as wind and sunlight, are typically used to generate electricity for residential users and small industries. Both types of power generation use ac/ac and dc/ac static PWM converters for voltage conversion and battery banks for long term energy storage. These converters perform maximum power point tracking to extract the maximum energy possible from wind and sun. The electrical energy consumption behaviour is random and unpredictable, and therefore, it may be single or three-phase, balanced or unbalanced, and linear or nonlinear. An active power filter is connected in parallel at the point of common coupling to compensate current harmonics, current unbalance, and reactive power. It is composed by an electrolytic capacitor, a four-leg PWM converter, and a first-order output ripple filter, as shown in Figure 2. This circuit considers the power system equivalent impedance Z_s, the converter output ripple filter impedance Z_f, and the load impedance Z_L. The four-leg PWM converter topology is shown in Figure 3.

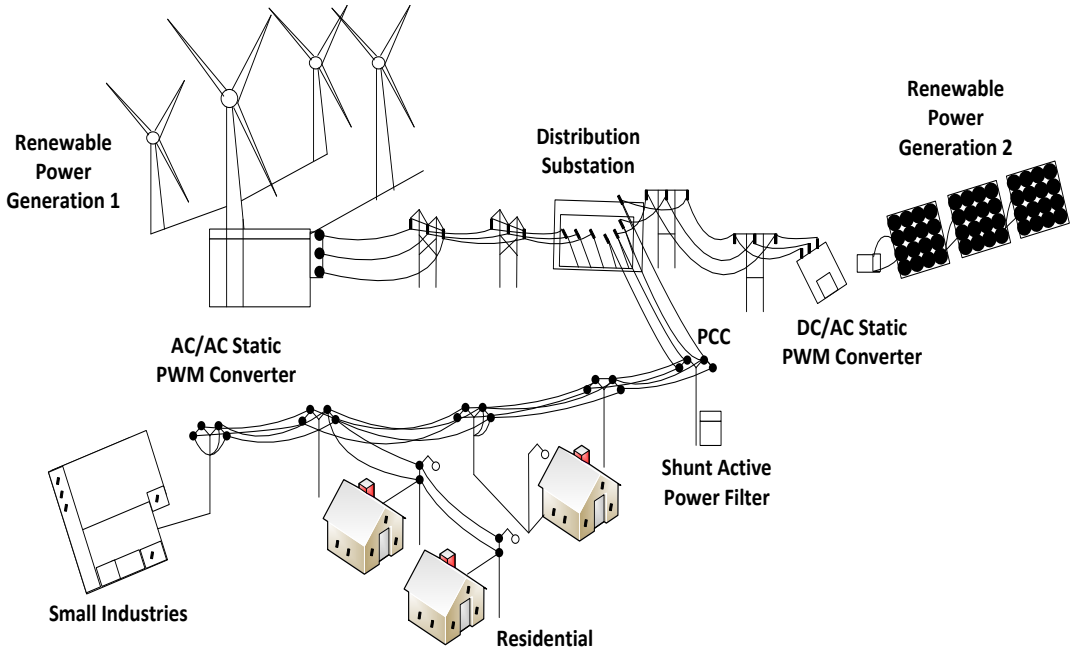

Figure 1. Stand-alone Hybrid Power Generation System with a Shunt Active Power Filter

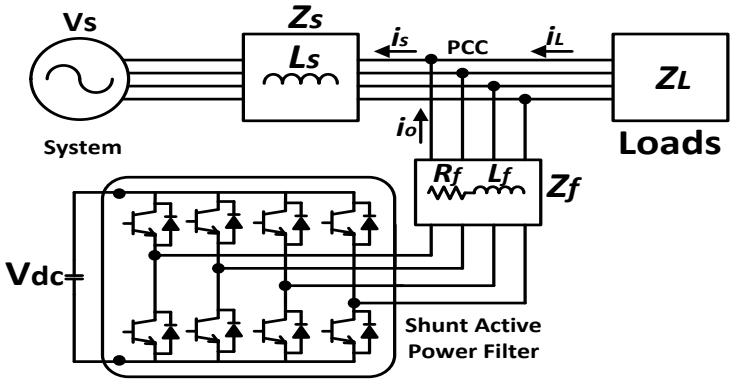

Figure 2. Three-phase Equivalent Circuit of the Proposed Shunt Active Power Filter

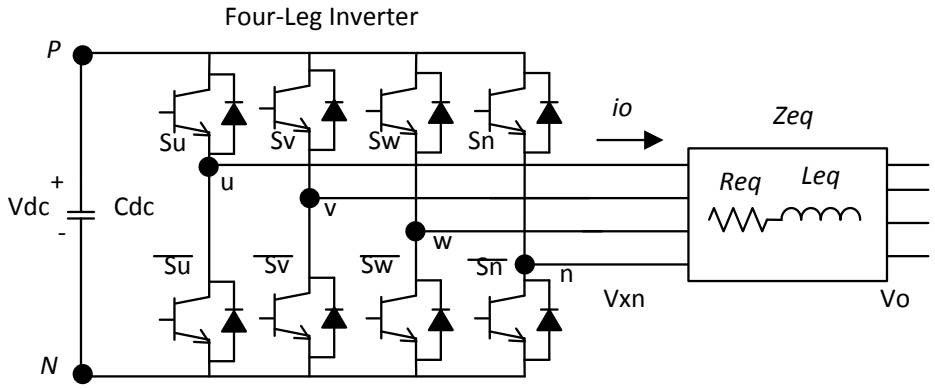

Figure 3. Two-level Four-leg PWM-VSI Topology

This converter topology is similar to the conventional three-phase converter with the fourth leg connected to the neutral bus of the system. The fourth leg increases switching states from 8 (2^3) to 16 (2^4), improving control flexibility and output voltage quality [21]-[32], and is suitable for current unbalanced compensation. The voltage in any leg x of the converter, measured from the neutral point (n), can be expressed in terms of switching states, as follows

$$v_{xn} = S_x - S_n v_{dc} \qquad \text{x = u, v, w, n} \tag{1}$$

The mathematical model of the filter derived from the equivalent circuit shown in Figure 2 is

$$V_0 = v_{xn} - R_{eq} i_0 - L_{eq} \frac{di_0}{dt} \tag{2}$$

where R_{eq} and L_{eq} are the 4L-VSI output parameters expressed as Thevenin impedances at the converter output terminals Z_{eq}. Therefore, the Thevenin equivalent impedance is determined by a series connection of the ripple filter impedance Z_f and a parallel arrangement between the system equivalent impedance Z_s and the load impedance Z_L

$$Z_{eq} = \frac{Z_s Z_L}{Z_s + Z_L} + Z_f \;;\; Z_s + Z_f \tag{3}$$

For this model, it is assumed that $Z_L \geq Z_s$, that the resistive part of the system's equivalent impedance is neglected, and that the series reactance is in the range of 3–7% p.u., which is an acceptable approximation of the real system. Finally, in (2) $R_{eq} = R_f$ and $L_{eq} = L_s + L_f$.

3. DIGITAL PREDICTIVE CURRENT CONTROL

The block diagram of the proposed digital predictive current control scheme is shown in Figure 4. This control scheme is basically an optimization algorithm and, therefore, it has to be implemented in a microprocessor. Consequently, the analysis has to be developed using discrete mathematics in order to consider additional restrictions such as time delays and approximations [10],[22]–[27]. The main characteristic of predictive control is the use of the system model to predict the future behaviour of the variables to be controlled. The controller uses this information to select the optimum switching state that will be applied to the power converter, according to predefined optimization criteria. The predictive control algorithm is easy to implement and to understand, and it can be implemented with three main blocks as shown in Figure 4.

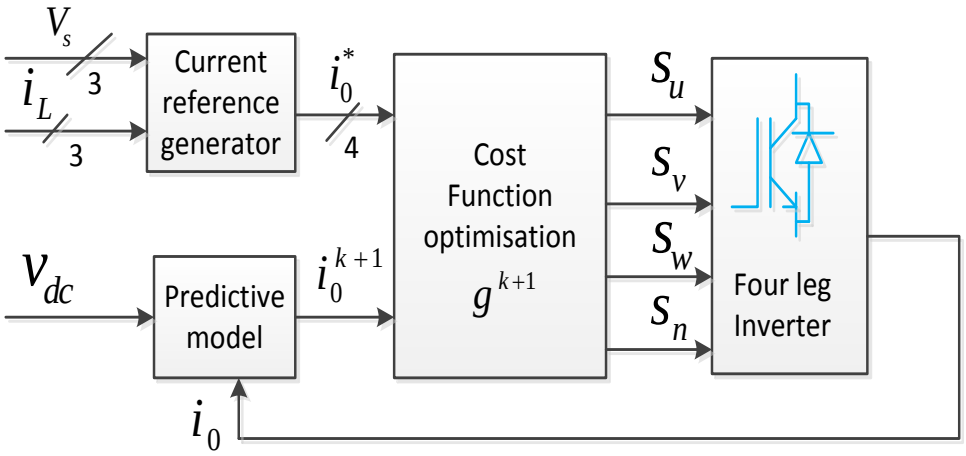

Figure 4. Proposed Predictive Digital Current Control Block Diagram

1) Current Reference Generator: This unit is designed to generate the required current reference that is used to compensate the undesirable load current components. In this case, the system voltages, the load currents, and the dc-voltage converter are measured, while the neutral output current and neutral load current are generated directly from these signals (IV).

2) Prediction Model: The converter model is used to predict the output converter current. Since the controller operates in discrete time, both the controller and the system model must be represented in a discrete time domain [22]. The discrete time model consists of a recursive matrix equation that represents this prediction system. This means that for a given sampling time T_s, knowing the converter switching states and control variables at instant kT_s, it is possible to predict the next states at any instant $[k + 1]$ Ts .Due to the first-order nature of the state equations that describe the model in (1)–(2), a sufficiently accurate first-order approximation of the derivative is considered in this paper.

$$\frac{dx}{dt} = \frac{x[k+1] - x[k]}{T_s} \tag{4}$$

The 16 possible output current predicted values can be obtained from (2) and (4) as

$$i_0[k+1] = \frac{T_s}{L_{eq}}(v_{xn}[k] - v_0[k]) + (1 - \frac{R_{eq}T_s}{L_{eq}})i_0[k] \tag{5}$$

As shown in (5), in order to predict the output current i_0 at the instant (k + 1), the input voltage value v_0 and the converter output voltage v_{xN}, are required. The algorithm calculates all 16 values associated with the possible combinations that the state variables can achieve.

3) Cost Function Optimization: In order to select the optimal switching state that must be applied to the power converter, the 16 predicted values obtained for $i_0[k + 1]$ are compared with the reference using a cost function g, as follows:

$$g[k+1] = (i_{ou}^*[k+1] - i_{ou}[k+1])^2 + (i_{ov}^*[k+1] - i_{ov}[k+1])^2 + (i_{ow}^*[k+1] - i_{ow}[k+1])^2 + (i_{on}^*[k+1] - i_{on}[k+1])^2 \quad (6)$$

The output current i_0 is equal to the reference (i_o^*) when g = 0. Therefore, the optimization goal of the cost function is to achieve a g value close to zero. The voltage vector v_{xN} that minimizes the cost function is chosen and then applied at the next sampling state. During each sampling state, the switching state that generates the minimum value of g is selected from the 16 possible function values. The algorithm selects the switching state that produces this minimal value and applies it to the converter during the k + 1 state.

4. CURRENT REFERENCE GENEREATION

A *dq*-based current reference generator scheme is used to obtain the active power filter current reference signals. This scheme presents a fast and accurate signal tracking capability. This characteristic avoids voltage fluctuations that deteriorate the current reference signal affecting compensation performance [28]. The current reference signals are obtained from the corresponding load currents as shown in Figure 5.

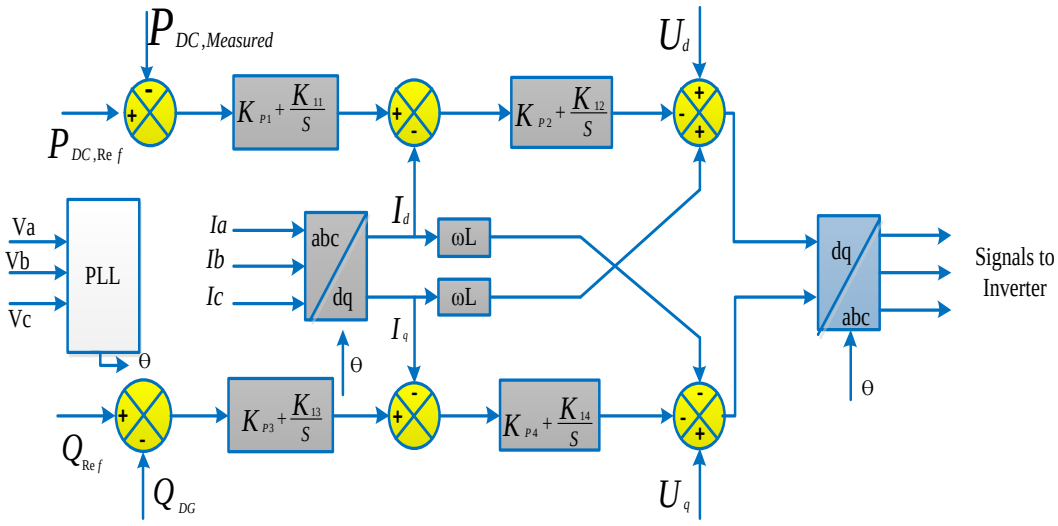

Figure 5. *dq*-based Current Reference Generator Block Diagram

This module calculates the reference signal currents required by the converter to compensate reactive power, current harmonic and current imbalance. The displacement power factor (sin $\varphi_{(L)}$) and the maximum total harmonic distortion of the load (THD $_{(L)}$) defines the relationships between the apparent power required by the active power filter, with respect to the load, as shown

$$\frac{S_{APF}}{S_L} = \frac{\sqrt{\sin\Phi_{(L)} + THD_{(L)}^2}}{\sqrt{1 + THD_{(L)}^2}} \quad (7)$$

where the value of THD $_{(L)}$ includes the maximum compensable harmonic current, defined as double the sampling frequency f_s. The frequency of the maximum current harmonic component that can be compensated is equal to one half of the converter switching frequency.

The dq-based scheme operates in a rotating reference frame; therefore, the measured currents must be multiplied by the sin (ωt) and cos (ωt) signals. By using dq-transformation, the d current component is synchronized with the corresponding phase-to-neutral system voltage, and the q current component is phase-shifted by 90°. The sin (ωt) and cos (ωt) synchronized reference signals are obtained from a synchronous reference frame (SRF) PLL [29]. The SRF-PLL generates a pure sinusoidal waveform even when the system voltage is severely distorted. Tracking errors are eliminated, since SRF-PLLs are designed to avoid phase voltage unbalancing, harmonics (i.e., less than 5% and 3% in fifth and seventh, respectively), and offset caused by the nonlinear load conditions and measurement errors [30]. Equation (8) shows the relationship between the real currents i_{Lx} (t) (x = u, v, w) and the associated dq components (i_d and i_q).

$$\begin{bmatrix} i_d \\ i_q \end{bmatrix} = \sqrt{\frac{2}{3}} \begin{bmatrix} \sin\omega t & \cos\omega t \\ -\cos\omega t & \sin\omega t \end{bmatrix} \begin{bmatrix} 1 & -\frac{1}{2} & -\frac{1}{2} \\ 0 & \frac{\sqrt{3}}{2} & -\frac{\sqrt{3}}{2} \end{bmatrix} \begin{bmatrix} i_{Lu} \\ i_{Lv} \\ i_{Lw} \end{bmatrix} \tag{8}$$

A low-pass filter (LFP) extracts the dc component of the phase currents id to generate the harmonic reference components i_d. The reactive reference components of the phase-currents are obtained by phase-shifting the corresponding ac and dc components of i_q by 180◦. In order to keep the dc-voltage constant, the amplitude of the converter reference current must be modified by adding an active power reference signal i_e with the d-component, as will be explained in Section IV-A. The resulting signals i_d^* and i_q^* are transformed back to a three phase system by applying the inverse Park and Clark transformation, as shown in (9). The cut off frequency of the LPF used in this paper is 20 Hz

$$\begin{bmatrix} i_{ou}^* \\ i_{ov}^* \\ i_{ow}^* \end{bmatrix} = \sqrt{\frac{2}{3}} \begin{bmatrix} \frac{1}{\sqrt{2}} & 1 & 0 \\ \frac{1}{\sqrt{2}} & -\frac{1}{2} & \frac{\sqrt{3}}{2} \\ \frac{1}{\sqrt{2}} & -\frac{1}{2} & -\frac{\sqrt{3}}{2} \end{bmatrix} \times \begin{bmatrix} 1 & 0 & 0 \\ 0 & \sin\omega t & -\cos\omega t \\ 0 & \cos\omega t & \sin\omega t \end{bmatrix} \begin{bmatrix} i_0 \\ i_d^* \\ i_q^* \end{bmatrix} \tag{9}$$

The current that flows through the neutral of the load is compensated by injecting the same instantaneous value obtained from the phase-currents, phase-shifted by 180^0, as shown next

$$i_{on}^* = -(i_{Lu} + i_{Lv} + i_{Lw}) \tag{10}$$

One of the major advantages of the dq-based current reference generator scheme is that it allows the implementation of a linear controller in the dc-voltage control loop. However, one important disadvantage of the dq-based current reference frame algorithm used to generate the current reference is that a second order harmonic component is generated in i_d and i_q under unbalanced operating conditions. The amplitude of this harmonic depends on the percent of unbalanced load current (expressed as the relationship between the negative sequence current $i_{L,2}$ and the positive sequence current $i_{L,1}$. The second-order harmonic cannot be removed from i_d and i_q, and therefore generates a third harmonic in the reference current when it is converted back to abc frame [31]. Figure 6 shows the percent of system current imbalance and the percent of third harmonic system current, in function of the percent of load current imbalance. Since the load current does not have a third harmonic, the one generated by the active power filter flows to the power system.

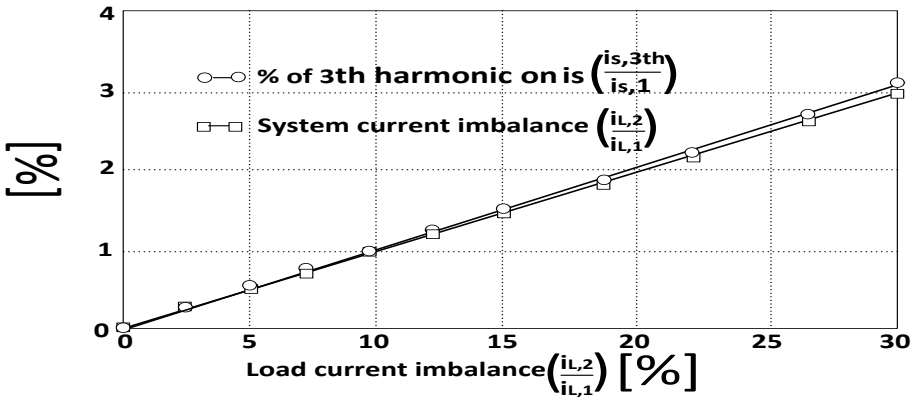

Figure 6. Relationship between Permissible Unbalance Load Currents, the Corresponding Third-order Harmonic Content, and System Current Imbalance (with Respect to Positive Sequence of the System Current, $i_{s,1}$)

4.1. DC-Voltage Control

The dc-voltage converter is controlled with a traditional PI controller. This is an important issue in the evaluation, since the cost function (6) is designed using only current references, in order to avoid the use of weighting factors. Generally, these weighting factors are obtained experimentally, and they are not well defined when different operating conditions are required. Additionally, the slow dynamic response of the voltage across the electrolytic capacitor does not affect the current transient response. For this reason, the PI controller represents a simple and effective alternative for the dc-voltage control. The dc-voltage remains constant (with a minimum value of $\sqrt{6}\ v_{s\,(rms)}$) until the active power absorbed by the converter decreases to a level where it is unable to compensate for its losses.

The active power absorbed by the converter is controlled by adjusting the amplitude of the active power reference signal i_e , which is in phase with each phase voltage. In the block diagram shown in Figure 5, the dc-voltage v_{dc} is measured and then compared with a constant reference value v_{dc}^* . The error (e) is processed by a PI controller, with two gains, K_p and T_i. Both gains are calculated according to the dynamic response requirement. Figure 7 shows that the output of the PI controller is fed to the dc-voltage transfer function G_s, which is represented by a first-order system (11)

$$G(s) = \frac{v_{dc}}{i_e} = \frac{3}{2}\frac{K_p v_s \sqrt{2}}{C_{dc} v_{dc}^*} \tag{11}$$

The equivalent closed-loop transfer function of the given system with a PI controller (12) is shown in (13)

$$C(s) = K_p(1 + \frac{1}{T_i.s}) \tag{12}$$

$$\frac{v_{dc}}{i_e} = \frac{\frac{\omega_n^2}{a}.(s+a)}{s^2 + 2\delta\omega_n.s + \omega_n^2} \tag{13}$$

Since the time response of the dc voltage control loop does not need to be fast, a damping factor ζ = 1 and a natural angular speed $\omega_n = 2\pi \cdot 100$ rad/s are used to obtain a critically damped response with minimal voltage oscillation. The corresponding integral time $T_i = 1/a$ (13) and proportional gain K_p can be calculated as

$$\delta = \sqrt{\frac{3}{8}\frac{K_p v_s \sqrt{2} T_i}{C_{dc} v_{dc}^*}} \quad (14)$$

$$\omega_n = \sqrt{\frac{3}{2}\frac{K_p v_s \sqrt{2}}{C_{dc} v_{dc}^* T_i}} \quad (15)$$

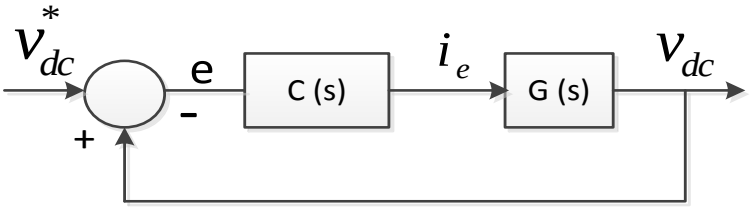

Figure 7. DC-Voltage Control Block Diagram

5. SIMULATION RESULTS

A simulation model for the three-phase four-leg PWM converter with the parameters shown in Table I has been developed using MATLAB-Simulink. The objective is to verify the current harmonic compensation effectiveness of the proposed control scheme under different operating conditions. A six-pulse rectifier was used as a nonlinear load. The proposed predictive control algorithm was programmed using an S-function block that allows simulation of a discrete model that can be easily implemented in a real-time interface (RTI) on the dSPACE DS1103 R&D control board. Simulations were performed considering a 20 [μs] of sample time. In the simulated results shown in Figure 8, the active filter starts to compensate at $t = t_1$. At this time, the active power filter injects an output current i_{ou} to compensate current harmonic components, current unbalanced, and neutral current simultaneously. During compensation, the system currents i_s show sinusoidal waveform, with low total harmonic distortion (THD = 3.93%). At $t = t_2$, a three-phase balanced load step change is generated from 0.6 to 1.0 p.u. The compensated system currents remain sinusoidal despite the change in the load current magnitude. Finally, at $t = t_3$, a single-phase load step change is introduced in phase u from 1.0 to 1.3 p.u., which is equivalent to an 11% current imbalance. As expected on the load side, a neutral current flow through the neutral conductor (i_{Ln}), but on the source side, no neutral current is observed (i_{sn}). Simulated results show that the proposed control scheme effectively eliminates unbalanced currents. Additionally, Figure 8 shows that the dc-voltage remains stable throughout the whole active power filter operation.

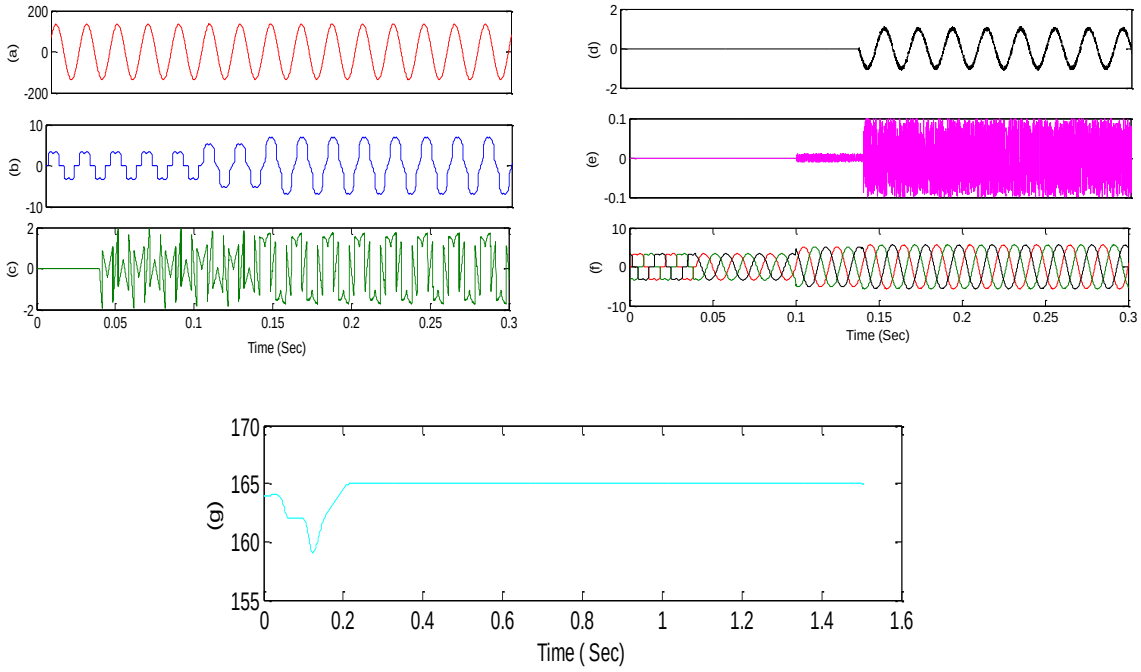

Figure 8. Simulated Waveforms of the Proposed Control Scheme (a) Phase to Neutral Source Voltage, (b) Load Current, (c) Active Power Filter Output Current, (d) Load Neutral Current, (e) System Neutral Current, (f) System Currents, (g) DC Voltage Converter

6. EXPERIMENTAL RESULTS

The compensation effectiveness of the active power filter is corroborated in a 2 kVA experimental setup. A six-pulse rectifier was selected as a nonlinear load in order to verify the effectiveness of the current harmonic compensation. A step load change was applied to evaluate the transient response of the dc voltage loop. Finally, an unbalanced load was used to validate the performance of the neutral current compensation. Because the experimental implementation was performed on a dSPACE I/O board, all I/O Simulink blocks used in the simulations are 100% compatible with the dSPACE system capabilities. The complete control loop is executed by the controller every 20 μs, while the selected switching state is available at 16 μs. An average switching frequency of 4.64 kHz is obtained.

Figure 9 shows the transient response of the compensation scheme. Figure 9(a) shows that the line current becomes sinusoidal when the active power filter starts compensation, and the dc-voltage behaves as expected. (b) Voltage and system waveforms, v_{su} and i_{su} , i_{sv} , $i_{sw.}$ Consequence good tracking characteristic of the current references, as shown in Figure 9(d). In Figure 10, the transient response of the active power filter under a step load change is shown. The line currents remain sinusoidal and the dc-voltage returns to its reference with a typical transient response of an under damped second-order system (maximum overshoot of 5% and two cycles of settling time). In this case, a step load change is applied from 0.6 to 1.0 p.u. Finally, the load connected to phase u was increased from 1.0 to 1.3 p.u. The corresponding waveforms are shown in Figure 11. Figure 11(a) shows that the active filter is able to compensate the current in the neutral conductor with fast transient response Moreover, Figure 11(b) shows that the system neutral current *i*on is effectively compensated and eliminated, and system currents remain balanced even if an 11% current imbalance is applied.

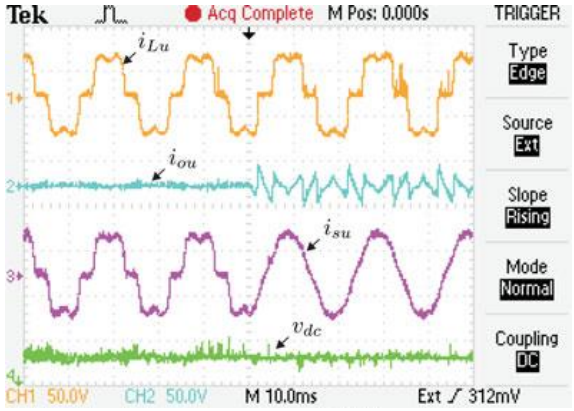

(a)

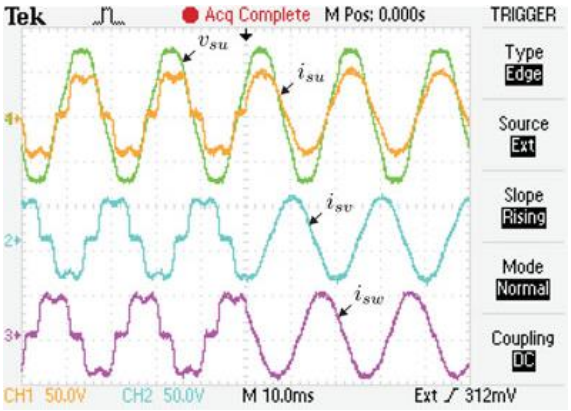

(b)

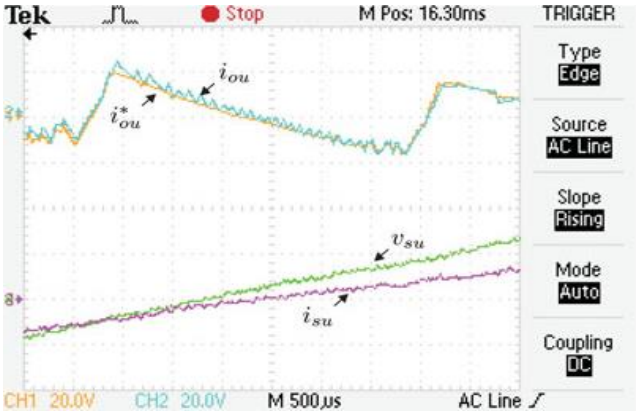

(c)

Figure 9. Experimental Transient Response after APF Connection. (a) Load Current i_{Lu} , active power filter current i_{ou} , dc-voltage converter $v$dc , and system current i_{su} . Associated frequency spectrum. (b) Voltage and system waveforms, v_{su} and i_{su}, i_{sv}, i_{sw} (c) Current reference signals i^*_{ou} , and active power filtercurrent i_{ou} (tracking characteristic).

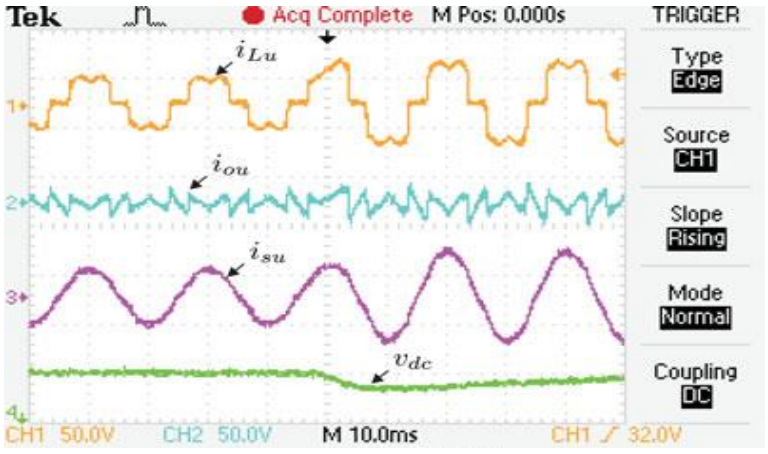

Figure 10. Experimental Results for Step Load Change (0.6 to 1.0 p.u.). Load Current i_{Lu} , active power filter current i_{ou} , system current i_{su} , and dc-voltage converter v_{dc}

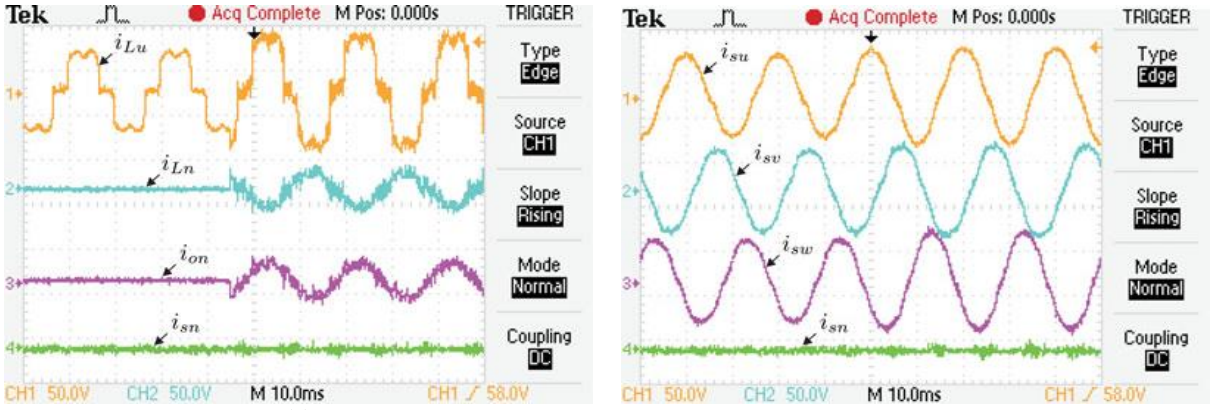

Figure 11. Experimental Results for Step Unbalanced Phase u Load Change (1.0 to 1.3 p.u.) (a) Load Current i_{Lu}, load neutral current i_{Ln}, active power filter neutral current i_{on}, and system neutral current isn, (b) System currents i_{su}, i_{sv}, i_{sw}, and i_{sn}

7. CONCLUSION

Improved dynamic current harmonics and a reactive power compensation scheme for power distribution systems with generation from renewable sources has been proposed to improve the current quality of the distribution system. Advantages of the proposed scheme are related to its simplicity, modelling, and implementation. The use of a predictive control algorithm for the converter current loop proved to be an effective solution for active power filter applications, improving current tracking capability, and transient response. Simulated and experimental results have proved that the proposed predictive control algorithm is a good alternative to classical linear control methods. The predictive current control algorithm is a stable and robust solution. Simulated and experimental results have shown the compensation effectiveness of the proposed active power filter.

ACKNOWLEDGEMENTS

I express my thanks to the support given by management in completing my project. I also express my sincere gratitude & deep sense of respect to Dr. K S Srikanth for making us available all the required assistance & for his support & inspiration to carry out this project in the Institute. I would like to thank Dr. K S Srikanth, professor who has been an inspiring guide and committed faculty who gave relief moral support in every situation of engineering career. The encouragement and support by him, especially in carrying out this project motivated me to complete this project. I am thankful to the teaching and non-teaching staff of EEE department for their direct as well as indirect help in my project. I am elated to avail my selves to this opportunity to express my deep sense of gratitude to my parents.

REFERENCES

[1] R. Mo and H. Li, "Hybrid Energy Storage System with Active Filter Function for Shipboard MVDC System Applications Based on Isolated Modular Multilevel DC/DC Converter," in *IEEE Journal of Emerging and Selected Topics in Power Electronics*, vol/issue: 5(1), pp. 79-87, 2017.

[2] S. Ghosh, *et al.*, "Distribution Voltage Regulation through Active Power Curtailment with PV Inverters and Solar Generation Forecasts," in *IEEE Transactions on Sustainable Energy*, vol/issue: 8(1), pp. 13-22, 2017.

[3] M. Abarzadeh and H. M. Kojabadi, "A Static Ground Power Unit Based on the Improved Hybrid Active Neutral-Point-Clamped Converter," in *IEEE Transactions on Industrial Electronics*, vol/issue: 63(12), pp. 7792-7803, 2016.

[4] M. Abarzadeh, *et al.*, "A Modified Static Ground Power Unit Based on Novel Modular Active Neutral Point Clamped Converter," in *IEEE Transactions on Industry Applications*, vol/issue: 52(5), pp. 4243-4256, 2016.

[5] S. G. Vennelaganti, *et al.*, "Adaptable voltage source inverter for grid integration of renewables with enhanced power quality capabilities," *2016 IEEE International Conference on Industrial Technology (ICIT)*, Taipei, pp. 1242-1247, 2016.

[6] N. Eghtedarpour and E. Farjah, "Distributed charge/discharge control of energy storages in a renewable energy based DC micro-grid," in *IET Renewable Power Generation*, vol/issue: 8(1), pp. 45-57, 2014.

[7] S. Dhar and P. K. Dash, "Performance analysis of a new fast negative sequence power injection oriented islanding detection technique for photovoltaic photovoltaic based voltage source converter based micro grid operation," in *IET Generation, Transmission & Distribution*, vol/issue: 9(15), pp. 2079-2090, 2015.
[8] A. Kahrobaeian and Y. A. R. I. Mohamed, "Robust Single-Loop Direct Current Control of LCL-Filtered Converter-Based DG Units in Grid-Connected and Autonomous Microgrid Modes," in *IEEE Transactions on Power Electronics*, vol/issue: 29(10), pp. 5605-5619, 2014.
[9] P. H. Divshali, *et al.*, "Decentralized Cooperative Control Strategy of Microsources for Stabilizing Autonomous VSC-Based Microgrids," in *IEEE Transactions on Power Systems*, vol/issue: 27(4), pp. 1949-1959, 2012.
[10] A. Kahrobaeian and Y. A. R. I. Mohamed, "Robust Single-Loop Direct Current Control of LCL-Filtered Converter-Based DG Units in Grid-Connected and Autonomous Microgrid Modes," in *IEEE Transactions on Power Electronics*, vol/issue: 29(10), pp. 5605-5619, 2014.
[11] A. Milczarek, "Harmonic power sharing between power electronics converters in islanded AC microgrid," *2017 Progress in Applied Electrical Engineering (PAEE)*, Koscielisko, pp. 1-7, 2017.
[12] C. Gayithri and R. Dhanalakshmi, "Analysis of power quality on a renewable energy micro grid conversion system with current and power controller," *2016 International Conference on Advanced Communication Control and Computing Technologies (ICACCCT)*, Ramanathapuram, pp. 449-453, 2016.
[13] W. Kohn, *et al.*, "A Micro-Grid Distributed Intelligent Control and Management System," in *IEEE Transactions on Smart Grid*, vol/issue: 6(6), pp. 2964-2974, 2015.
[14] M. Davari and Y. A. R. I. Mohamed, "Robust Multi- Objective Control of VSC-Based DC-Voltage Power Port in Hybrid AC/DC Multi-Terminal Micro-Grids," in *IEEE Transactions on Smart Grid*, vol/issue: 4(3), pp. 1597-1612, 2013.
[15] L. A. d. S. Ribeiro, *et al.*, "Isolated Micro-Grids with Renewable Hybrid Generation: The Case of Lençóis Island," in *IEEE Transactions on Sustainable Energy*, vol/issue: 2(1), pp. 1-11, 2011.
[16] A. Kahrobaeian and Y. A. R. I. Mohamed, "Interactive Distributed Generation Interface for Flexible Micro-Grid Operation in Smart Distribution Systems," in *IEEE Transactions on Sustainable Energy*, vol/issue: 3(2), pp. 295-305, 2012.
[17] P. Shamsi and B. Fahimi, "Stability Assessment of a DC Distribution Network in a Hybrid Micro-Grid Application," in *IEEE Transactions on Smart Grid*, vol/issue: 5(5), pp. 2527-2534, 2014.
[18] M. E. S. Ahmed, *et al.*, "Two-stage micro-grid inverter with high-voltage gain for photovoltaic applications," in *IET Power Electronics*, vol/issue: 6(9), pp. 1812-1821, 2013.
[19] P. Yang and A. Nehorai, "Joint Optimization of Hybrid Energy Storage and Generation Capacity with Renewable Energy," in *IEEE Transactions on Smart Grid*, vol/issue: 5(4), pp. 1566-1574, 2014.
[20] A. Trivedi and M. Singh, "Repetitive Controller for VSIs in Droop-Based AC-Microgrid," in *IEEE Transactions on Power Electronics*, vol/issue: 32(8), pp. 6595-6604, 2017.
[21] B. D. Reddy, *et al.*, "Design, Operation, and Control of S3 Inverter for Single-Phase Microgrid Applications," in *IEEE Transactions on Industrial Electronics*, vol/issue: 62(9), pp. 5569-5577, 2015.
[22] L. Chen and S. Mei, "An integrated control and protection system for photovoltaic microgrids," in *CSEE Journal of Power and Energy Systems*, vol/issue: 1(1), pp. 36-42, 2015.
[23] D. Voglitsis, *et al.*, "Incorporation of Harmonic Injection in an Interleaved Flyback Inverter for the Implementation of an Active Anti-Islanding Technique," in *IEEE Transactions on Power Electronics*, vol/issue: 32(11), pp. 8526-8543, 2017.
[24] M. Prodanovic and T. C. Green, "Control and filter design of three-phase inverters for high power quality grid connection," in *IEEE Transactions on Power Electronics*, vol/issue: 18(1), pp. 373-380, 2003.
[25] Z. Zeng, *et al.*, "Multi-objective control of multi-functional grid-connected inverter for renewable energy integration and power quality service," in *IET Power Electronics*, vol/issue: 9(4), pp. 761-770, 2016.
[26] Rocabert, *et al.*, "Control of power converters in AC microgrids," *IEEE Trans. Power Electron.*, vol/issue: 27(11), pp. 4734-4749, 2012.
[27] M. Aredes, *et al.*, "Three-phase four- wire shunt active filter control strategies," *IEEE Trans. Power Electron.*, vol/issue: 12(2), pp. 311-318, 1997.
[28] S. Naidu and D. Fernandes, "Dynamic voltage restorer based on a fourleg voltage source converter," *Gener. Transm. Distrib, IET*, vol/issue: 3(5), pp. 437-447, 2009.
[29] N. Prabhakar and M. Mishra, "Dynamic hysteresis current control to minimize switching for three-phase four-leg VSI topology to compensate nonlinear load," *IEEE Trans. Power Electron.*, vol/issue: 25(8), pp. 1935-1942, 2010.
[30] V. Khadkikar, *et al.*, "Digital signal processor implementation and performance evaluation of split capacitor, four-leg and three h-bridge-based three-phase four-wire shunt active filters," *Power Electron., IET*, vol/issue: 4(4), pp. 463-470, 2011.
[31] F. Wang, *et al.*, "Grid-interfacing converter systems with enhanced voltage quality for microgrid application; concept and implementation," *IEEE Trans. Power Electron.*, vol/issue: 26(12), pp. 3501-3513, 2011.
[32] X.Wei, "Study on digital pi control of current loop in active power filter," in *Proc. 2010 Int. Conf. Electr. Control Eng.*, pp. 4287-4290, 2010.
[33] R. d. A. Ribeiro, *et al.*, "A robust adaptive control strategy of active power filters for power-factor correction, harmonic compensation, and balancing of nonlinear loads," *IEEE Trans.Power Electron.*, vol/issue: 27(2), pp. 718-730, 2012.
[34] J. Rodriguez, *et al.*, "Predictive current control of a voltage source inverter," *IEEE Trans. Ind. Electron.*, vol/issue: 54(1), pp. 495-503, 2007.

[35] P. Cortes, *et al.*, "Model predictive control of an inverter with output *LC* filter for UPS applications," *IEEE Trans. Ind Electron.*, vol/issue: 56(6), pp. 1875-1883, 2009.
[36] R. Vargas, *et al.*, "Predictive control of a three-phase neutral-point-clamped inverter," *IEEE Trans. Ind. Electron.*, vol/issue: 54(5), pp. 2697-2705, 2007.
[37] P. Cortes, *et al.*, "Modelpredictive control ofmultilevel cascaded H-bridge inverters," *IEEE Trans.Ind. Electron*, vol/issue: 57(8), pp. 2691-2699, 2010.
[38] P. Lezana, *et al.*, "Model predictive control ofan asymmetric flying capacitor converter," *IEEE Trans. Ind. Electron.*, vol/issue: 56(6), pp. 1839-1846, 2009.
[39] P. Correa, *et al.*, "A predictive controlscheme for current-source rectifiers," *IEEE Trans. Ind. Electron.*, vol/issue: 56(5), pp. 1813-1815, 2009.
[40] M. Rivera, *et al.*, "Currentcontrol for an indirect matrix converter with filter resonance mitigation," *IEEE Trans. Ind. Electron.*, vol/issue: 59(1), pp. 71-79, 2012.
[41] P. Correa, *et al.*, "Predictive torque control for inverter-fed induction machines," *IEEE Trans.Ind. Electron*, vol/issue: 54(2), pp. 1073-1079, 2007.
[42] M. Odavic, *et al.*, "Onesample-period-ahead predictive current control for high-performance active shunt power filters," *Power Electronics, IET*, vol/issue: 4(4), pp. 414-423, 2011.
[43] *IEEE Recommended Practice for Electric Power Distribution for IndustrialPlants*, IEEE Standard 141-1993, 1994.
[44] R. d. A. Ribeiro, *et al.*, "A robust adaptive control strategy of active power filters for power-factor correction, harmonic compensation, and balancing of nonlinear loads," *IEEE Trans. Power Electron.*, vol/issue: 27(2), pp. 718-730, 2012.
[45] M. Sumner, *et al.*, "A technique for power supply harmonic impedance estimation using a controlled voltage disturbance," *IEEE Trans. Power Electron.*, vol/issue: 17(2), pp. 207-215, 2002.
[46] S. Ali and M. Kazmierkowski, "PWM voltage and current control of four-leg VSI," presented at the ISIE, Pretoria, South Africa, vol. 1, pp. 196-201, 1998.
[47] S. Kouro, *et al.*, "Model predictive control-A simple and powerful method to control power converters," *IEEE Trans. Ind. Electron.*, vol/issue: 56(6), pp. 1826-1838, 2009.
[48] D. Quevedo, *et al.*, "Model predictive control of an AFE rectifier with dynamic references," *IEEE Trans. Power Electron.*, vol/issue: 27(7), pp. 3128-3136, 2012.
[49] Z. Shen, *et al.*, "Predictive digital current control of single-inductor multiple-output converters in CCM with low cross regulation," *IEEE Trans. Power Electron.*, vol/issue: 27(4), pp. 1917-1925, 2012.
[50] M. Rivera, *et al.*, "Predictive current control with input filter resonance mitigation for a direct matrix converter," *IEEE Trans. Power Electron.*, vol/issue: 26(10), pp. 2794-2803, 2011.
[51] M. Preindl and S. Bolognani, "Model predictive direct speed control with finite control set of PMSM drive systems," *IEEE Trans. Power Electron.*, 2012.
[52] T. Geyer, "Computationally efficient model predictive direct torque control," *IEEE Trans. Power Electron.*, vol/issue: 26(10), pp. 2804-2816, 2011.
[53] M. I. M. Montero, *et al.*, "Comparison of control strategies for shunt active power filters in three-phase four-wire systems," *IEEE Trans. Power Electron.*, vol/issue: 22(1), pp. 229-236, 2007.
[54] S. K. Chung, "A phase tracking system for three phase utility interface inverters," *IEEE Trans. Power Electron*, vol/issue: 15(3), pp. 431-438, 2000.
[55] M. K. Ghartemani, *et al.*, "Addressing DC component in PLL and notch filter algorithms," *IEEE Trans. Power Electron.*, vol/issue: 27(1), pp. 78-86, 2012.
[56] L. Czarnecki, "On some misinterpretations of the instantaneous reactive power p-q theory," *IEEE Trans. Power Electron.*, vol/issue: 19(3), pp. 828-836, 2004.
[57] S. Srikanth, "A Three Phase Multi Level Converter for grid Connected PV System," *International Journal of Power Electronics and Drive Systems*, vol/issue: 5(1), pp. 71-75, 2014.
[58] S. Srikanth, "Improvement of power quality using fuzzy logic controller in grid connected photovoltaic cell using UPQC," *International Journal of Power Electronics and Drive Systems*, vol/issue: 5(1), pp. 101-111, 2014.

BIOGRAPHIES OF AUTHORS

Dr. K.S Srikanth was born in Kakinada, Andhra Pradesh, India in the year 1980. He was awarded B.Tech EEE degree in the year 1999 from Chennai University. He was awarded M.Tech Instrumentation degree in the year 2001 from Andhra University. He was awarded Ph.D degree in the year 2010 from Andhra University. He has 13 years of teaching experience. He is currently working as professor in the department of Electrical and Electronics Engineering, Koneru Lakshmaiah University, Vijayawada, Andhra Pradesh, India.

Mr S Guru Prasad is a student passed out from JNTU Hyderabad from EEE Department. He obtained B.Tech degree from JNTU Hyderabad in 2006 and M.Tech degree from JNTU Hyderabad in 2008, Hyderabad. He had worked in different capacities in technical institiutions of higher learning over 10 years. He is currently working as Hod in Mekapati Rajamohan Reddy institute of Technology and science, Udayagiri. His current research includes Renewable energy and batteries.

Mr B V Rajanna is a student passed out from KL University from EEE Department. He obtained B.Tech degree from JNTU Kakinada in 2010 and M.Tech degree from KL University in 2015, Guntur. He had worked in different capacities in technical institiutions of higher learning over 3 years. He has over 9 publications in International Journals. His Current Research includes AMR(Automatic Meter Reading) devices, Smart Metering and Smart Grids, Dynamic Modeling of Batteries, Micro-Grids, Renewable Energy Sources, GSM/GPRS and PLC (Power Line Carrier) Communication and Various modulation techniques such as QPSK, BPSK, ASK, FSK, OOK and GMSK.